

CFD computations of the second round of MEXICO rotor measurements

This content has been downloaded from IOPscience. Please scroll down to see the full text.

2016 J. Phys.: Conf. Ser. 753 022054

(<http://iopscience.iop.org/1742-6596/753/2/022054>)

View [the table of contents for this issue](#), or go to the [journal homepage](#) for more

Download details:

IP Address: 130.112.1.3

This content was downloaded on 20/10/2016 at 14:37

Please note that [terms and conditions apply](#).

You may also be interested in:

[Rotor thermal stress monitoring in steam turbines](#)

Bouberle Antonín, Jakl Jan and Liška Jindich

[Dynamics of the interaction between the rotor and the induction zone](#)

Mahmood Mirzaei, Alexander R. Meyer Forsting and Niels Trolborg

[Quantum to Classical Transition in a System of Two Coupled Kicked Rotors](#)

Zhao Wen-Lei and Jie Quan-Lin

[Stall-Induced Vibrations of the AVATAR Rotor Blade](#)

M Stettner, M J Reijerkerk, A Lünenschloß et al.

[Simulations of wind turbine rotor with vortex generators](#)

Niels Trolborg, Frederik Zahle and Niels N. Sørensen

[Finding the ideal strategy: Full-scale fatigue testing of wind turbine rotor shafts](#)

T Rauert, J Herrmann, P Dalhoff et al.

[Uncertainty propagation in CFD using polynomial chaos decomposition](#)

O M Knio and O P Le Maître

CFD computations of the second round of MEXICO rotor measurements

Niels N. Sørensen¹, F. Zahle¹, K. Boorsma², G. Schepers²

¹ DTU Wind Energy, Technical University of Denmark, Risø Campus, Denmark.

² Energy Research Center of the Netherlands, ECN, P.O. Box 1, 1755 ZG Petten Holland.

E-mail: nsqr@dtu.dk

Abstract. A comparison, between selected wind tunnel data from the NEW MEXICO measuring campaign and CFD computations are shown. The present work, documents that a state of the art CFD code, including a laminar turbulent transition model, can provide good agreement with experimental data. Good agreement is shown for the integral loads, radial distributions of blades forces, pressure distributions, and the velocity profiles up- and downstream of the rotor.

1. Introduction

The development, application, and acceptance of CFD solvers for wind turbine rotor flows have been greatly dependent on the availability of good experimental data under controlled conditions. The NREL/NASA AMES Wind Tunnel Experiment in 1999 [3, 14] might be the most well known. Other series of wind tunnel experiments exist, and the Swedish experiment in the Chinese CARDC tunnel, performed in 1989 and 1992 [12] and [11], is an early example. Here, the focus is on the recent NEW MEXICO campaign of measurements of the MEXICO rotor, performed within the European INNWIND project, and relying on European ESWIRP project for wind tunnel time. One obvious feature, of both the MEXICO [15] and NEW MEXICO measurements [2], is the fact that this specific experiment encompasses both detailed rotor load measurements on the wind turbine blades and simultaneous detailed PIV measurements in the wake behind the rotor. Another unique feature of the NEW MEXICO experiment is the availability of both natural and tripped flow conditions, allowing investigation of the effect of laminar/turbulent transition. This proved important in the original MEXICO experiment, [13], where the simultaneous availability of loads and wake measurements revealed inconsistency between loads and wake deficit. In the new measurements, a large effort is put into revealing the cause of this issue [2]. The original MEXICO experiment has spawned a long row of computational studies, as reported e.g. in [1, 10, 4, 5, 16]

An important aspect, addressed in the new experiment, is the laminar/turbulent transition process. In the original experiment, the blades were equipped with boundary layer trips, to assure fully turbulent flow at the relatively low Reynolds numbers present in the wind tunnel setup. In the second round of measurements, the effect of running the outer part of the blade with free transition is investigated, due to the increasing focus on the transition process for wind turbine flows.



2. Method

In this work, the EllipSys3D incompressible CFD solver is applied in RANS mode, [7, 8, 18]. The turbulent closure is accomplished by the $k-\omega$ SST turbulence model of Menter [6]. For the laminar turbulent transitional computations the $k-\omega$ SST model is used in combination with the E^n method, as implemented by Michelsen [9]. In the present simulation, the intermittency constant is overwritten on the inboard part of the rotor, to enforce fully turbulent flow. All the present simulations deal with axial flow situations and are computed using a steady state approach.

3. Grid Generation

The Mexico rotor is a three bladed upwind turbine, with a rotor diameter of 4.5 meters. The rotor is equipped with DU-91-W2-250 airfoils at the inboard part of the blades, Risø-A21 at the central part, and NACA 64-418 airfoils on the outer part, see [15, 13]. The turbine is equipped with five rows of pressure tabs, at $r/R=[0.25, 0.35, 0.60, 0.82, 0.92]$, to allow determination of the span-wise load distribution.

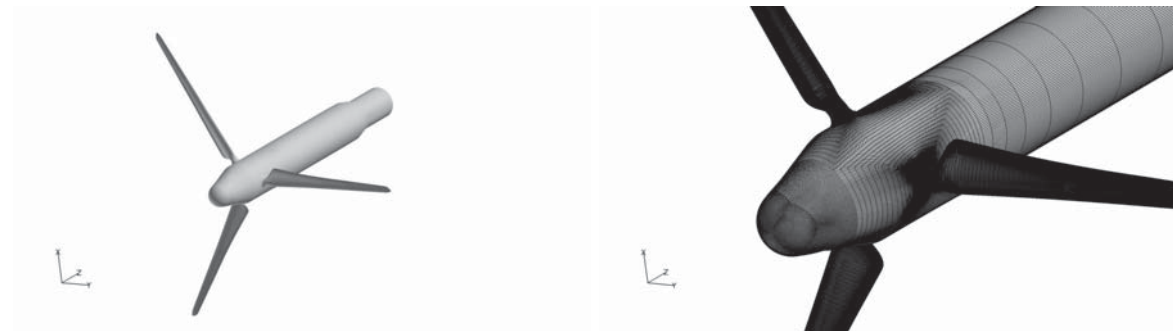


Figure 1. The three bladed MEXICO rotor, with the substantial nacelle geometry. The left figure shows the geometry and the right figure shows mesh details.

Table 1. The operational conditions for the three investigated cases.

CASE	V_{tunnel} [m/s]	RPM	Pitch [deg]	Density [kg/m ³]	T_{inf} [deg K]	P_{inf} [N/m ²]
1	10.05	425.1	-2.3	1.197	293.63	101398
2	15.06	425.1	-2.3	1.191	294.91	101345
3	24.05	425.1	-2.3	1.195	294.25	101407

Based on a CAD description of the MEXICO blade and nacelle a surface grid is generated by an in-house surface grid generation library, while the 3D grid is generated by a 3D in-house hyperbolic grid generator. In contrast to previous computations, using the EllipSys3D code for the MEXICO setup, the substantial turbine nacelle is included in the computations, see Figure 1. The mesh has 129 cells in the span-wise direction, 256 cells in the chord-wise direction, and 128 cells in the normal direction. In the normal direction the wall normal cell size is 1×10^{-5} meter, which assures an y^+ below 2. The far-field boundary is placed 10 diameters away from the rotor center in all direction. The effect of including the substantial nacelle will not be discussed in detail as this is not the main focus of the work. A brief comparison of fully turbulent results revealed that the presence of the nacelle increase the power and the axial load by approximately

Table 2. The integral loads for the three considered cases, giving the axial force and shaft torque for experimental exp , the computed results for transitional conditions Ell,tr , and the computed results for fully turbulent conditions Ell,ft .

CASE	$F_{axial,exp}$ [N]	$F_{axial,Ell,tr}$ [N]	$F_{axial,Ell,ft}$ [N]	T_{exp} [Nm]	$T_{Ell,tr}$ [Nm]	$T_{Ell,ft}$ [Nm]
1	974	984	969	68	58	59
2	1663	1752	1704	317	285	278
3	2173	2494	2532	716	704	727

1-2 percent. The effect is much larger than should be expected for a full size turbine, where the nacelle is much smaller compared to the rotor area.

4. Results

In the present paper, a comparison of selected experimental conditions in axial flow is compared to computations, see Table 1.

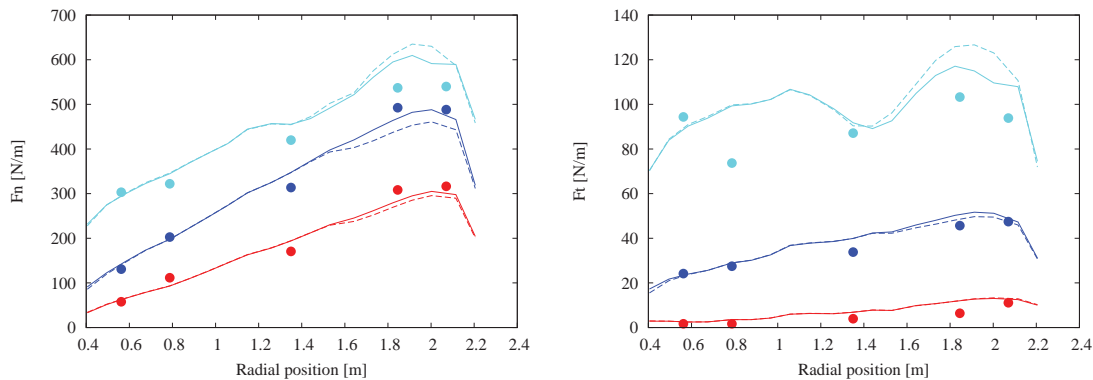


Figure 2. Radial load distributions for the three considered cases. The left figure shows the normal loads and the right figure the tangential loads. The experiments are shown with symbols, the fully turbulent computations with lines, and the transitional conditions with dashed lines. The red, blue, and green color corresponds to the $V_{tunnel} = 10, 15, \text{ and } 24$ [m/s] cases respectively.

The fully turbulent and transitional computations are compared with the measured data with respect to integral loads, span-wise force distributions, pressure distributions, and velocities in the wake of the turbine. The loads, in both the experiment and computations, are derived from the the five sectional pressure distributions by integration. The integration is based on a simple linear variation between the sections assuming zero value at the root and tip. As viscous friction contributions are not available in the experiment, friction is not included in the load determination from the CFD computations.

Looking first at the integral loads, we see that in comparison with the old MEXICO measurements, taken under very similar conditions, the error in the thrust were varying as [18, 15, 10] percent, and the error in the torque is varying [20, 14, 6] percent for the [10, 15, 24] [m/s] cases. As seen in Table 2, the thrust error in the present comparison is reduced to [1, 5, 1.5] percent, while the error in the torque is reduced to [15, 10, 2] percent. As explained in the preliminary analysis of the New MEXICO measurements [2], the two main issues responsible

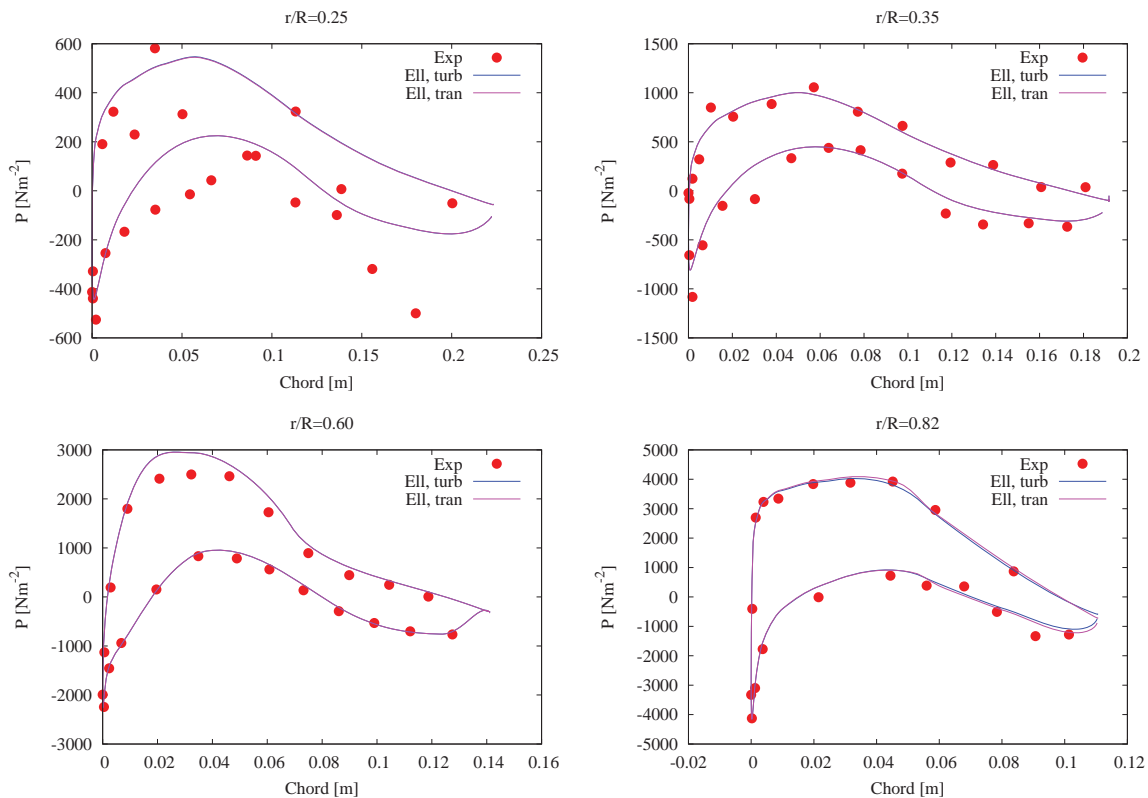


Figure 3. Pressure distributions at four span-wise sections for Case-1 (10 [m/s]), comparing the experimental values with fully turbulent and transitional computations.

for the mismatch of the loading and wake velocities, in the original MEXICO experiment, were an overestimation of the tunnel speed by approximately 0.2-0.3 [m/s] and under estimation of the loads, due to direct usage of the standard calibration curve provided by the manufacturer instead of individual calibration curves for the Kulite pressure measurement equipment. The present results, with a few percent error in the thrust and a somewhat higher error in the torque, agrees well with our general findings for typical CFD predictions of rotor flows. The highest error observed in the CASE-1 scenario is assumed to be connected to the conditions being close to vortex ring state.

The radial load distributions are shown in Figure 2 for the three considered cases. Compared to the old predictions, the agreement is improved, due to the removal of the consistent overestimation of the loads in the experiment, see Figure. 2. Additionally, it can be observed that the effect of the transition model is relatively weak, even though generally beneficial for the agreement.

The pressure distribution show very good agreement, see Figures 3 to 5, with the exception of the inboard sections at low wind speed, where it is known from [2] that the pressure sensors range is insufficient to resolve the actual physics.

The improved agreement of the computations are also observed in the velocity profiles. In the following, only the transitional results are shown, as the difference between the fully turbulent and transitional results are very minor. Starting with the axial transects of axial and tangential velocity, the computations show an excellent agreement both up- and down-stream of the rotor,

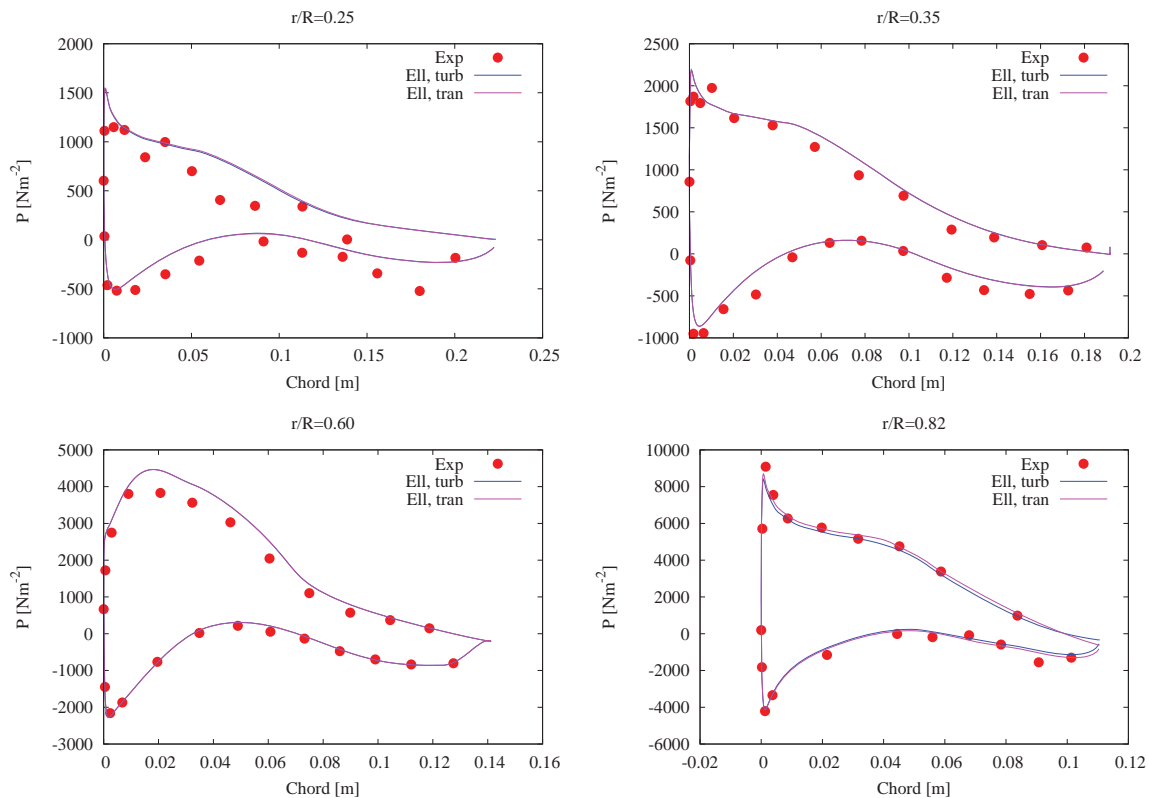


Figure 4. Pressure distributions at four span-wise sections for Case-2 (15 [m/s]), comparing the experimental values with fully turbulent and transitional computations.

see Figure 6. This is in contrast with the 'under prediction' in the old simulations, which were caused by an error in the measured tunnel speed.

Finally, Figures 7 to 9 show radial profiles of azimuthally averaged velocities. Here the computations show very good agreement with the measured profiles. In the old measurements, a light reflection from the turbine caused erroneous measurements of the axial velocity profile, see Figure 3 in [17]. The discussion, whether this feature existed or not, caused great debate in the modelling community, and it illustrates how combining measurements with computations can help gain physical understanding.

5. Conclusion

The present paper, illustrates the level of agreement which can typically be obtained between well executed controlled experiments and state of the art CFD computations, with respect to integral loads, span-wise load distributions, sectional pressure distributions, and wake velocities. The agreement is good, especially considering that the experiment features large separated areas for the highest wind speed. For the lowest wind speed the situation is close to vortex ring state, a very complicated flow situation where reversed flow regions exist in the wake region of the rotor. Additionally, it is discussed how the combination of experiments and computations can validate each other, making sure that the right conclusions are drawn with respect to the flow physics. The three present cases are only a small fraction of the measured cases from the New MEXICO campaign, and it is expected that the new data set will be very useful in connection

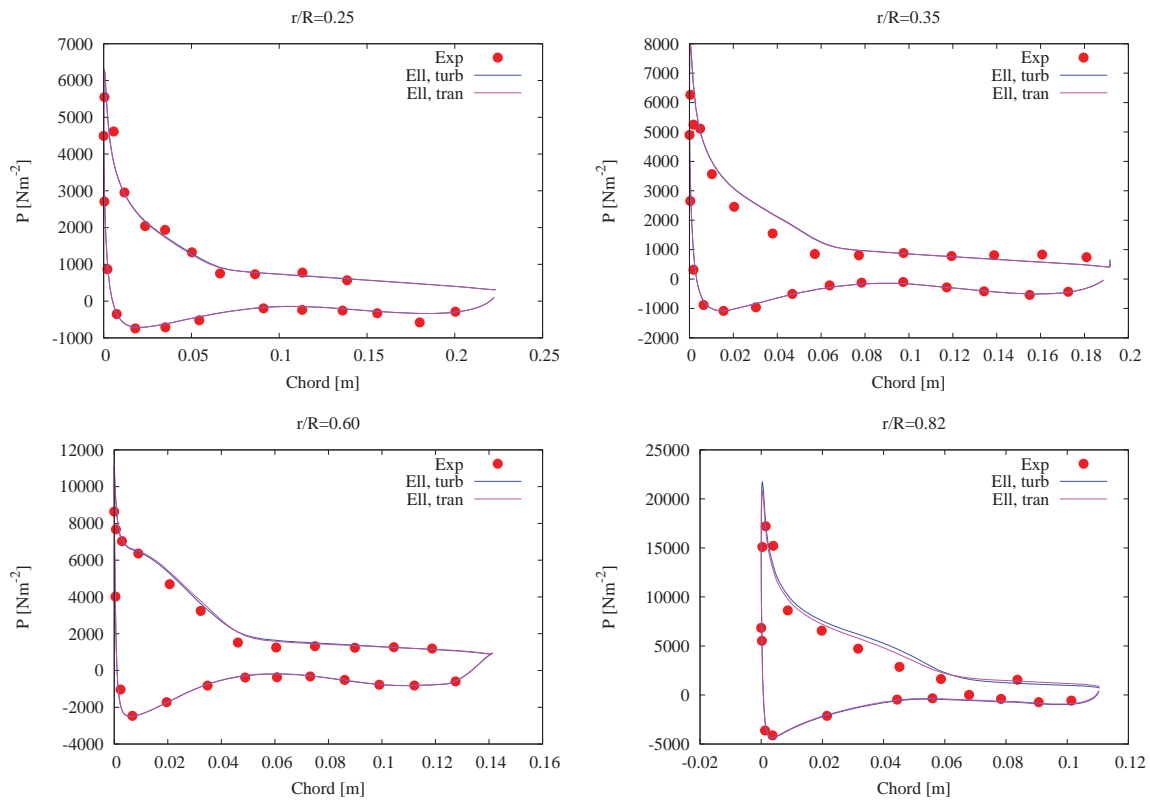


Figure 5. Pressure distributions at four span-wise sections for Case-3 (24 [m/s]), comparing the experimental values with fully turbulent and transitional computations.

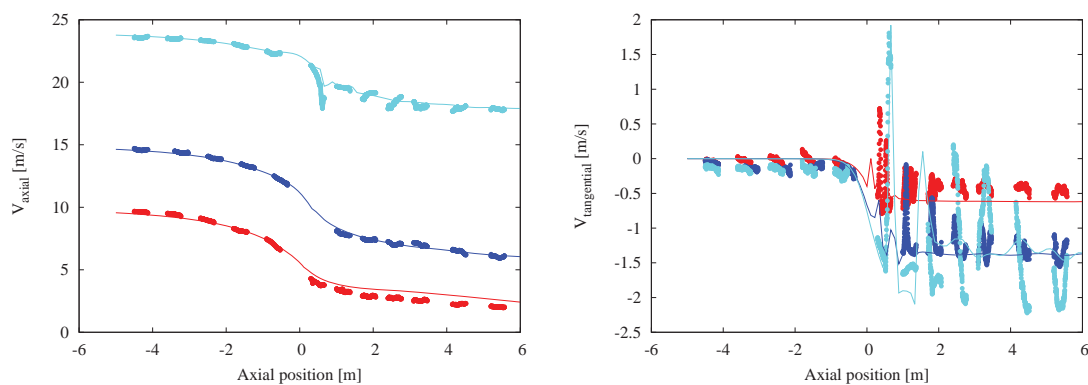


Figure 6. Velocity profiles along a line at $r=1.5$ [m], at the 9 o'clock position, with blade 1 pointing vertically up. The left figure shows the axial velocity and the right figure shows the tangential velocity. Only transitional conditions are shown.

with future flow solver validations and improvements.

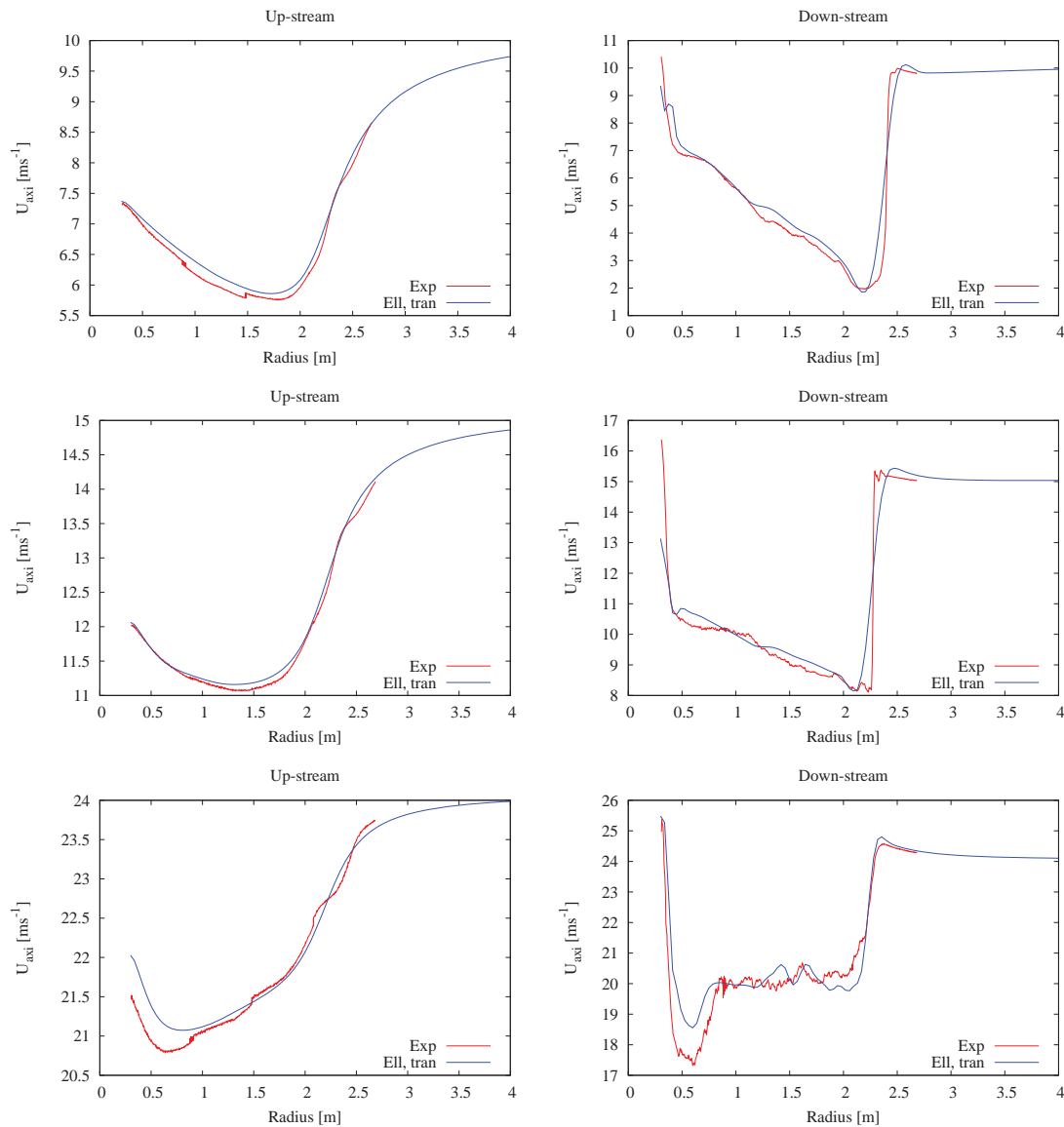


Figure 7. A comparison between measured and computed radial profiles of averaged axial velocity 0.3 [m] up- and down-stream of the rotor. From top to bottom V_{tunnel} is 10, 15, 24 [m/s]. Only the transitional results are shown.

5.1. Acknowledgments

The work is partially funded by the Danish Council for Strategic Research (DSF), under contract 2104-09-0026, Center for Computational Wind Turbine Aerodynamics and Atmospheric Turbulence, and by the Danish EUDP program, project title Dansk deltagelse i IEA Wind Task 29 Mexnext III, contract no. J.nr. 64014-0543. The computations are performed on the DTU PC-cluster JESS.

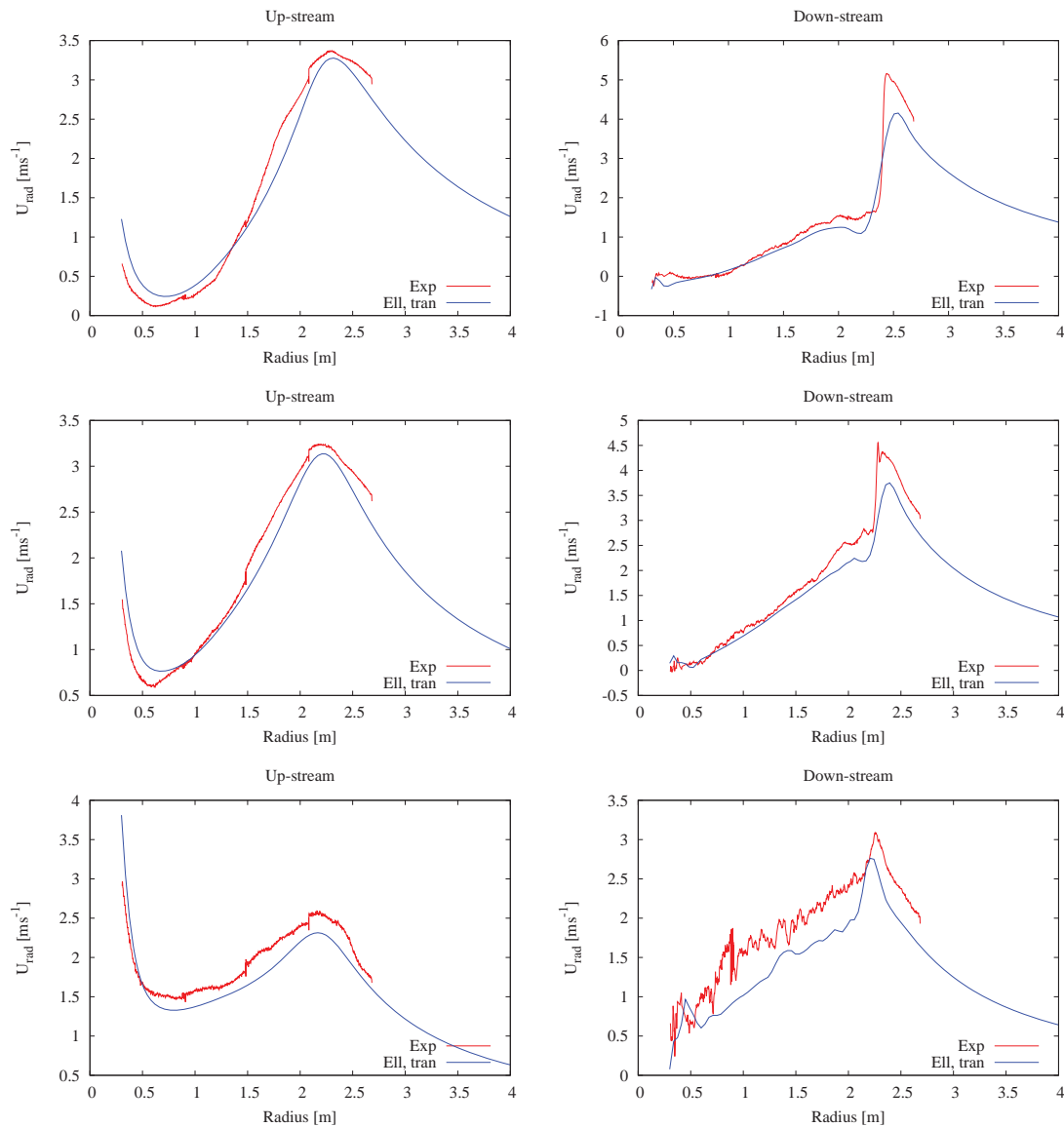


Figure 8. A comparison between measured and computed radial profiles of averaged radial velocity 0.3 [m] up- and down-stream of the rotor. From top to bottom V_{tunnel} is 10, 15, 24 [m/s]. Only the transitional results are shown.

6. References

- [1] A. Bechmann and N. N. Sørensen. CFD simulation of the MEXICO rotor wake. In *EWEC 2009 Scientific proceedings*, pages 64–68. EWEC, 2009. Presented at: 2009 European Wind Energy Conference and Exhibition : Marseille (FR), 16-19 Mar, 2009.
- [2] K. Boorsma and G. Schepers. New Mexico Experiment, Preliminary overview with initial validation. Technical report, Energy Research Center of the Netherlands, ECN, September 2014.
- [3] L. Fingersh, D. Simms, M. Hand, D. Jager, J. Cortrell, M. Robinsion, S. Schreck, and S. Larwood. Wind Tunnel Testing of NREL’s Unsteady Aerodynamics Experiment. In *2001 ASME Wind Energy Symposium*, pages 129–135, Reno, NV, January 11-14 2001. ASME. AIAA-2001-0035.
- [4] F. Grasso and A. Garrel. Near Wake Simulation of Mexico Rotor in Axial and Yawed Flow Conditions with

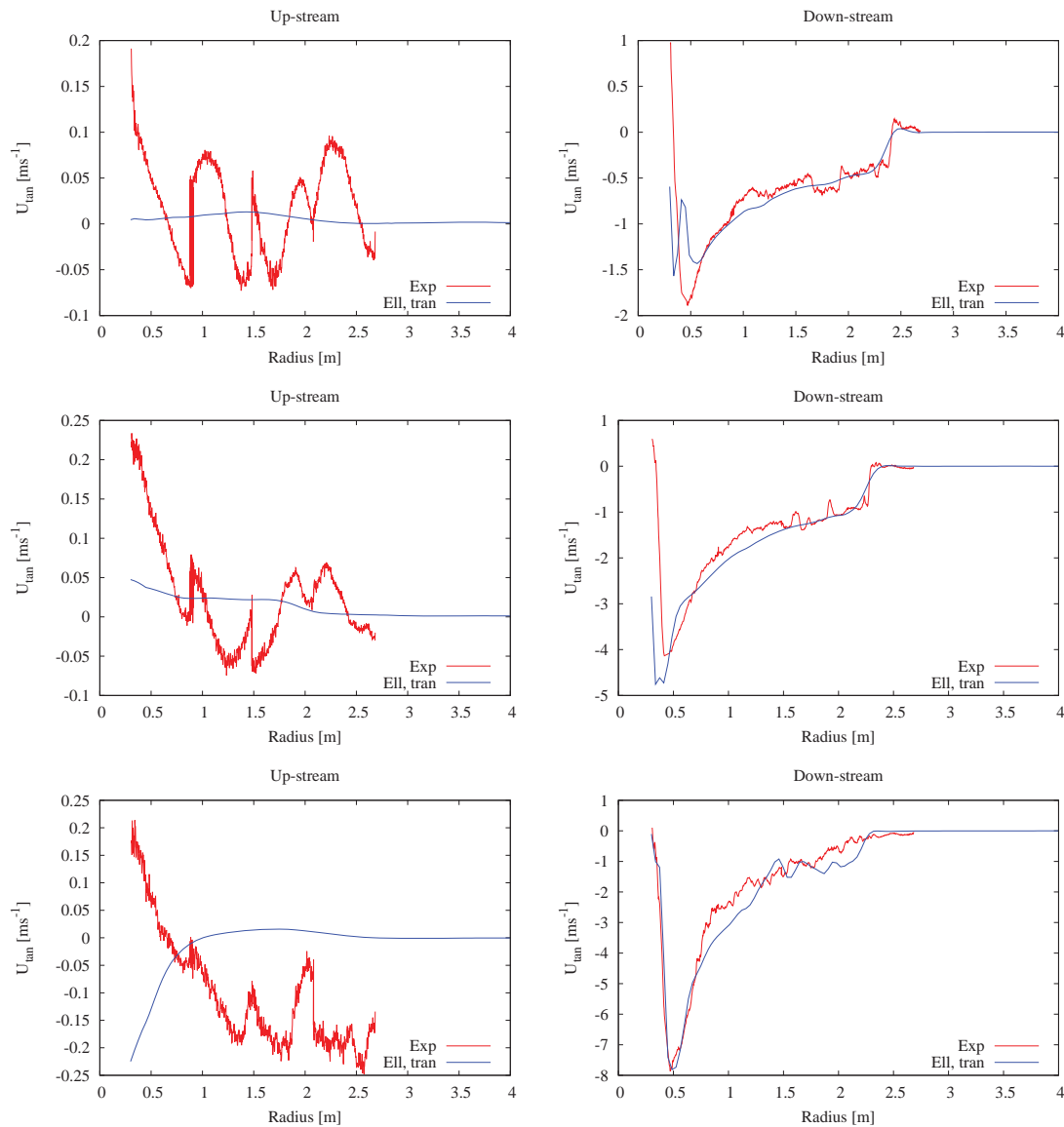


Figure 9. A comparison between measured and computed radial profiles of averaged tangential velocity 0.3 [m] up- and down-stream of the rotor. From top to bottom V_{tunnel} is 10, 15, 24 $[\text{m/s}]$. Only the transitional results are shown.

Lifting Line Free Wake Code. ECN-M-11-063, Energy Research Center of the Netherlands, P.O. Box 1, 1755 ZG Petten, 2011.

- [5] T. Lutz, K. Meister, and E. Krämer. Near Wake Studies of the MEXICO Rotor. In *EWEC 2011 Proceedings online*. EWEC, 2011. Presented at: 2011 European Wind Energy Conference and Exhibition: Brussels (BE), 14-17 Mar, 2011.
- [6] F. R. Menter. Zonal Two Equation $k-\omega$ Turbulence Models for Aerodynamic Flows. *AIAA paper 1993-2906*, 1993.
- [7] J. A. Michelsen. Basis3D - a Platform for Development of Multiblock PDE Solvers. Technical Report AFM 92-05, Technical University of Denmark, Department of Fluid Mechanics, Technical University of Denmark, December 1992.

- [8] J. A. Michelsen. Block structured Multigrid solution of 2D and 3D elliptic PDE's. Technical Report AFM 94-06, Technical University of Denmark, Department of Fluid Mechanics, Technical University of Denmark, May 1994.
- [9] J. A. Michelsen. *Forskning i aeroelasticitet EFP-2001*, chapter Beregning af laminar-turbulent omslag i 2D og 3D, page 73. Risø-R1349(DA). 2002. In Danish.
- [10] P.-E. M. Réthoré, N. N. Sørensen, F. Zahle, A. Bechmann, and H. Aagaard Madsen. Mexico Wind Tunnel and Wind Turbine modelled in CFD. In *AIAA Paper 2011-3373*. AIAA, 2011. Presented at: AIAA Fluid Dynamics Conference : Honolulu (US) 27-30 Jun, 2011.
- [11] G. Ronsten. Static pressure measurements on a rotating and a non-rotating 2.375 m wind turbine blade. Comparison with 2D computations. *J. of Wind Engineering and Industrial Aerodynamics*, 39:105–118, 1992.
- [12] G. Ronsten. Geometry and Installation in Wind Tunnels of a STORK 5.0 WPX Wind Turbine Blade Equipped with Pressure Taps. Technical Report FFAP-A 1006, 1994.
- [13] J. Schepers and H. Snel. Model Experiments in Controlled Conditions. ECN-E-07-042, Netherlands Energy Research Foundation, ECN, P.O. Box 1, 1755 ZG Petten, 2007.
- [14] D. Simms, S. Schreck, M. Hand, and L. J. Fingersh. NREL Unstead Aeorydnamics Experiment in the NASA-Ames Wind tunnel: A Comparison of Predictions to Measurements. NREL/TP -500-29494, Nat. Ren. Energy Lab., Golden, CO, 2001.
- [15] H. Snel, J. Schepers, and B. Montgomerie. The MEXICO project (Model Experiments in Controlled Conditions): The database and first results of data processing and interpretation. *J. Phys.: Conf. Ser.*, 75, 2007.
- [16] N. Sørensen, A. Bechmann, P.-E. Réthoré, and F. Zahle. Near wake Reynolds-averaged Navier–Stokes predictions of the wake behind the MEXICO rotor in axial and yawed flow conditions. *Wind Energy*, 17(1):75–86, 2014.
- [17] N. Sørensen, A. Bechmann, P.-E. Rthor, and F. Zahle. Near wake reynolds-averaged navierstokes predictions of the wake behind the mexico rotor in axial and yawed flow conditions. *Wind Energy*, 17(1):75–86, 2014.
- [18] N. N. Sørensen. General Purpose Flow Solver Applied to Flow over Hills. Risø-R- 827-(EN), Risø National Laboratory, Roskilde, Denmark, June 1995.